Hindawi Publishing Corporation
VLSI Design
Volume 2008, Article ID 291686, 8 pages
doi:10.1155/2008/291686

Research Article

MEMS Switches and SiGe Logic for Multi-GHz Loopback Testing

D. C. Keezer,[1] D. Minier,[2] P. Ducharme,[2] D. Viens,[2] G. Flynn,[3] and J. McKillop[3]

[1] *School of Electrical and Computer Engineering, Georgia Institute of Technology, Atlanta, GA 30332, USA*
[2] *IBM Canada, Bromont, Quebec, Canada J2L1A3*
[3] *TeraVicta Technologies, Austin, TX 78758, USA*

Correspondence should be addressed to D. C. Keezer, dkeezer@ece.gatech.edu

Received 17 October 2007; Accepted 23 January 2008

Recommended by José Machado da Silva

We describe the use of microelectromechanical system (MEMS) switches and SiGe logic devices for both passive and active loopback testing of wide data buses at rates up to 6.4 Gbps per signal. Target applications include HyperTransport, fully buffered DIMM, and PCI Express, among others. Recently introduced MEMS devices provide >7 GHz bandwidth in a very small package (needed to handle wide buses). SiGe logic supports >7 Gbps signals when active shaping of the waveform is required. Each loopback module typically supports between 9 and 16 differential channels. Multiple cards are used to handle applications with very wide buses or multiple ports. Passive cards utilize MEMS for switching between the loopback (self-test) mode and traditional automated test equipment (ATE) source/receiver channels. Future active card designs may provide additional waveform-shaping functions, such as buffering, amplitude attenuation/modulation, deskew, delay adjustment, jitter injection, and so forth. The modular approach permits precalibration of the loopback electronics and easy reconfiguration between debug or characterization testing and high-volume production screening.

1. INTRODUCTION

During the past few years we have developed a modular approach for production testing at multiple-GHz rates using conventional automated test equipment (ATE) [1–4]. The modules have included various configurations of "driver" and "receiver" channels that multiplex low-speed (<1 Gbps) ATE signals up to 6.4 Gbps as needed for device-under-test (DUT) testing. Some applications have required as many as 50–100 differential pair signals, each running at these multi-Gbps rates [4]. We have successfully applied this approach on two popular ATE platforms: (1) the Agilent/Verigy 93000-P1000 and (2) the Teradyne UltraFlex with "high-speed-digital" (HSD) and limited "serial-bus-6 GHz" (SB6G) channels.

In this paper, we extend the technique to loopback testing by introducing several new passive and active modules. We target two I/O standards including HyperTransport3 (HT3 at 5.2 Gbps) and fully-buffered dual in-line memory module (FB-DIMM at 4.8 Gbps). Section 2 describes a newly-developed microelectromechanical (MEMS) switch technology which is critical to the loopback solutions that are introduced in Section 3. A comparison of passive loopback modules using either miniature mechanical relays or MEMS is provided in Section 4. Active loopback solutions are shown in Section 5.

Loopback testing, illustrated in Figure 1, is a form of built-in self-test (BIST), whereby the device-under-test (DUT) contains appropriate logic to synthesize test signals which are transmitted through the DUT outputs, and are used to stimulate the DUT inputs. During loopback testing, the DUT outputs take the place of test signals which traditionally are supplied by the ATE. This greatly reduces the need for high-performance ATE resources for the loopback tests. Usually this type of testing requires minimal support from the ATE, so it is highly economical especially when testing high-speed devices.

However, loopback testing is only one of many types of tests that need to be applied to the DUT. For example, DC parametric tests (such as input leakage measurements, input and output voltage sensitivities, etc.) require direct connection of the ATE resources to the DUT I/O. Furthermore,

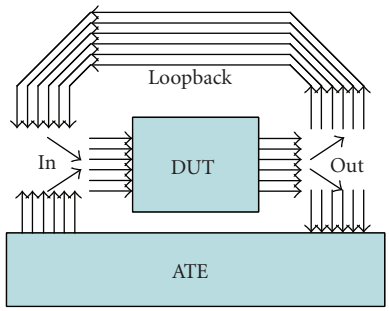

Figure 1: Loopback testing in an ATE test configuration.

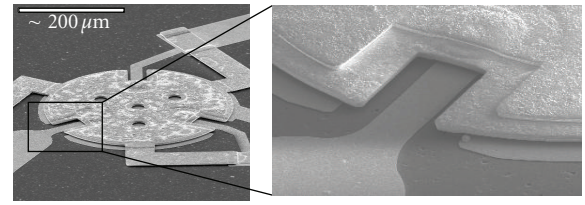

Figure 2: SEM photographs of the high force disk actuator (a) and details of the switch contact area (b).

loopback testing tends to be a pass/fail type test, so direct connections to the ATE are also required for functional diagnostic testing.

Since at least two connections are needed for each DUT I/O (one for loopback and one for traditional testing), and each must support a clean (stub-free) 50-Ohm transmission path, a high-performance switch is needed for each I/O. Logically, 2 : 1 multiplexers and 1 : 2 fanout buffers might be considered. However, a passive connection to the ATE is preferred so that DC parametric and AC waveform characteristics can be tested using traditional ATE resources. In this paper, we demonstrate the advantages of MEMS for this switching application.

2. MEMS SWITCH TECHNOLOGY

As in many testing applications, loopback tests require a way of switching between different signal sources and receivers. Specifically (as shown in Section 3), we need to switch between the ATE resources and the DUT I/O. The traditional approach is to use mechanical (or "reed" type relays). However, the large channel-counts and need for ultra-high bandwidth has forced the development of an even smaller technology called microelectromechanical systems (MEMS) switches. These have proven to be well suited to the loopback testing application, and represent a critical enabling technology for wide-bus applications above 3.2 Gbps (see the performance measurements in Sections 4 and 5).

Recently, TeraVicta has introduced a MEMS switch called TT712.The TT712 switch is fabricated using metal deposition processes found in most CMOS microelectronics manufacturing facilities. However, it also incorporates a number of proprietary features that enable both high performance and high reliability. The TT712 uses a unique device-on-package construction in which the MEMS device is fabricated directly onto the primary packaging material, in this case a ceramic (alumina) wafer with conductive metal vias. Individual switch features are patterned using conventional sputter deposition and etching processes with bulk metal layers (including the sacrificial material) fabricated via electroplating. A selective metal etch is used to remove this sacrificial metal layer (the "release" process), leaving the free standing MEMS switch structure. A scanning electron micrograph (SEM) is shown in Figure 2.

This "device-on-package" architecture has several significant benefits, especially in high-bandwidth test applications. First, the use of conductive vias minimizes the conduction paths within the device and between the device and the printed circuit board, directly reducing insertion loss and minimizing the length of radiating conductive elements that degrade high-frequency performance [5]. This, coupled with surface mount technology (SMT) compatible ball grid array (BGA) solder ball attachment, provides reliable, highly manufacturable signal connections that deliver chip-level high-frequency performance to the circuit board. The use of an alumina substrate also provides substantially lower high-frequency losses than the silicon substrates used in other MEMS switches [6]. This is especially true for devices operating at higher frequencies and for through-substrate via designs like the TT712.

Failures due to stiction between metal surfaces following removal of the sacrificial metal are minimized by key features of the proprietary high force disk actuator (HFDA). This uses a circular design to maximize contact stability and to restore force within the smallest possible footprint. This design also maximizes contact force (proportional to electrode area), which is a key factor in enabling low contact resistance (insertion loss) [7]. Contact stability is further optimized using a "three point" contact configuration, which helps assure that the force on the active electrical contact is highly uniform and repeatable. This results in a very low loss, highly repeatable contact configuration as shown.

The large restoring force of this design is required to provide reliable (stiction free) operation. Although this results in a relatively high switch voltage (68 V), low voltage operation (3–5 V) can be achieved through the use of a separate charge pump IC.

Switches with multiple contact configurations, such as single-pole-double-throw (SPDT) and double-pole-double-throw (DPDT) are constructed by connecting multiple HFDAs in a single package. This is illustrated by the solid model of the basic DC-7 GHz SPDT switch shown in Figure 3, which is shaded according to electric potential of the metal surface (darkest features corresponding to the highest field). The RF signal is conducted into the switch through a central terminal (RF common), which connects to two HFDAs on the device.

The package is carefully matched to 50-Ohm impedance throughout a very wide bandwidth. Typical RF performance of the DC-7 GHz SPDT switch is presented in Figure 4, and shows that these devices have insertion loss of less than 0.1 dB

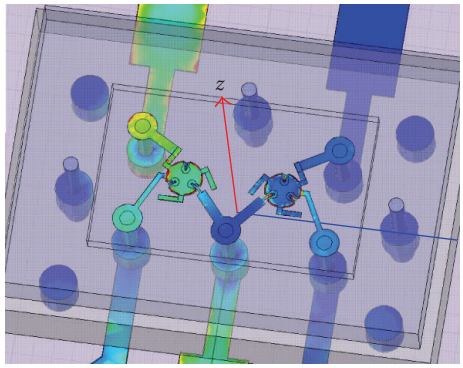

Figure 3: Ansoft model of the DC-7 GHz SPDT switch.

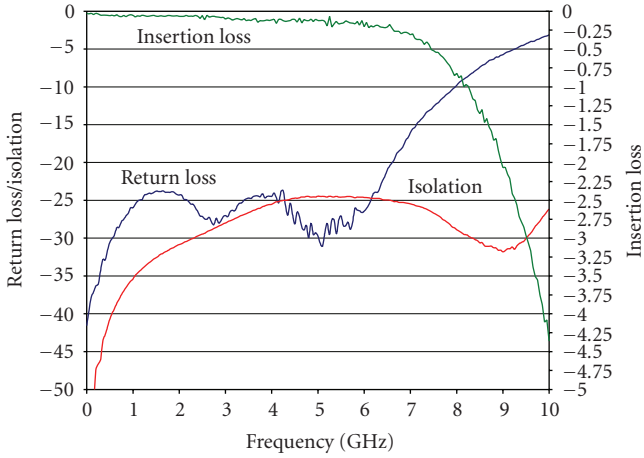

Figure 4: Typical RF performance of the DC-7 GHz SPDT switch.

at frequencies less than 1 GHz (<0.4 dB at 7 GHz), more than 20 dB of return loss and at least 25 dB of isolation. These devices are capable of switching up to 15 W of continuous RF power, with a peak power handling capability of at least 30 W.

In addition to the MEMS Switch's electrical and reliability advantages, there are two other very attractive features important for the loopback test application. First, the electrostatic nature of the actuator is inherently a low-power device, requiring an insignificant amount of current ($\ll$1 uA) to maintain the desired state. Therefore, there is negligible power dissipated within the switches of the loopback module. This feature reduces the cooling requirements. Even more important for large signal-count applications is the significantly smaller package size as compared with typical RF mechanical relays. This is illustrated in Figure 5. The MEMS package has a somewhat smaller footprint, but a *much* shorter height. This shorter dimension is a great advantage when designing thin loopback modules which permits the use of more modules to handle higher-density buses.

Notice that the footprint of the TT712 package is heavily dominated by the external connections. The internal switch elements account for a very small fraction of the device

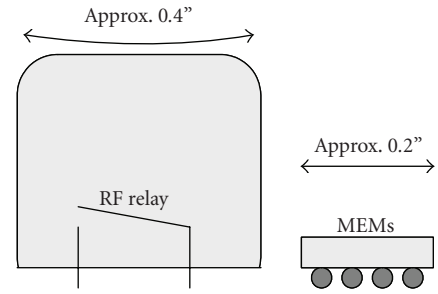

Figure 5: Size comparison of typical mechanical RF relay and MEMS switch packages.

footprint (as seen in Figure 3). Therefore, the MEMS technology has the potential to provide higher levels of integration and therefore support for much higher bus densities.

3. LOOPBACK MODULE DESIGNS

Fundamentally, the minimal loopback test requires that the DUT outputs be connected to appropriate DUT inputs as introduced in Figure 1, and shown in more detail in Figure 6. This allows the internal built-in self-test (BIST) circuits to generate test stimulus patterns for its own inputs, which are then analyzed by internal BIST circuitry as well. However, because we also need to do extensive DC parametric tests, as well as lower-speed functional tests, there must be an option to break the loopback path and substitute connections directly to/from the ATE (also shown in the figure). Switches (relays) are the obvious choice for this. However, great care is required in order to preserve signal integrity at multi-GHz rates.

The design of a suitable loopback module can leverage many of the features that we have previously applied to "driver" and "receiver" modules. For example, in the design of these earlier modules we have taken great care in selecting connectors, relays, and active components that can support the high bandwidth required for multi-GHz signals. We have also devised a common card configuration that fits within the physical constraints of the ATE testheads, while allowing for a maximum number of modules. In many test applications, the entire available volume located directly under the device-interface-board (DIB) is occupied by our modules.

Figure 7 shows a bottom view of a 2-slot DIB with one of our early 2-card loopback boards mounted in "Slot 1." This loopback board was specifically designed to be a direct "drop-in" replacement for a 9-channel HyperTransport driver module (8 data and a clock signal). In this application, Slot 2 (empty in the photo) normally holds a receiver module which likewise can be replaced with another loopback card. The two cards connect to one another through an array of coaxial connectors (upper right corner of the photo), thereby completing the connection of 9 differential pairs for the loopback test.

The cards have mechanical RF relays that allow the DUT I/O to either be connected in the loopack configuration or directly to ATE channels ("low speed" connections). This

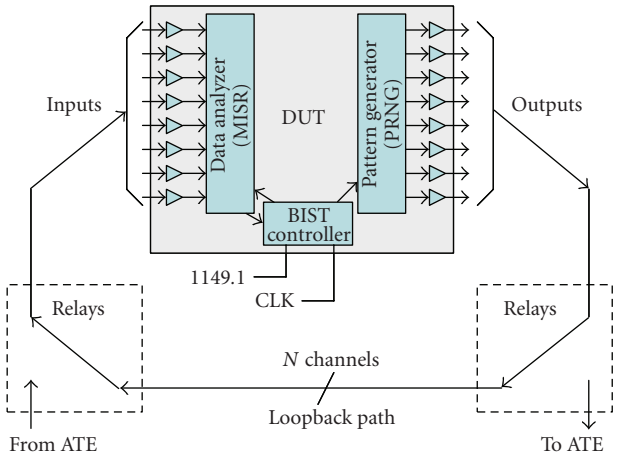

Figure 6: Minimum signal connection paths for loopback and switches to allow direct connection to ATE channels.

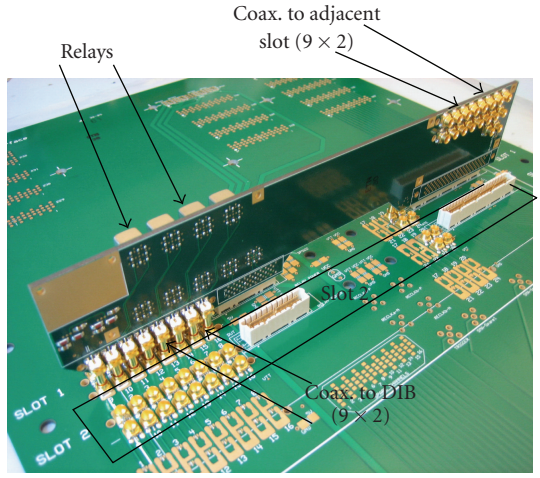

Figure 7: Nine-channel passive loopback card in a 2-slot configuration (slot 2 is empty). Bottom view of DIB.

arrangement is illustrated in Figure 8. In the figure the heavy dark arrows show the loopback path and also represent the coaxial connectors (which can be seen in Figure 7). The thinner lines/arrows show the "low speed" connections to/from the ATE.

In other designs (where drop-in compatibility was not required), we incorporated both the driver and receiver loopback switches onto a single card. This eliminates the card-to-card coaxial connections and reduces transmission line lengths. The "single-card" loopback arrangement is shown in Figure 9. Performance characteristics for each of these configurations are given in the following sections.

In order to remove heat and to tightly control the module temperature (for improved timing accuracy) we construct water-cooled heatsinks for each card. When using mechanical relays, the total module thickness is between 0.75 and 1.00 inch and is largely limited by the height of the relay packages. The use of MEMS switches not only reduces the

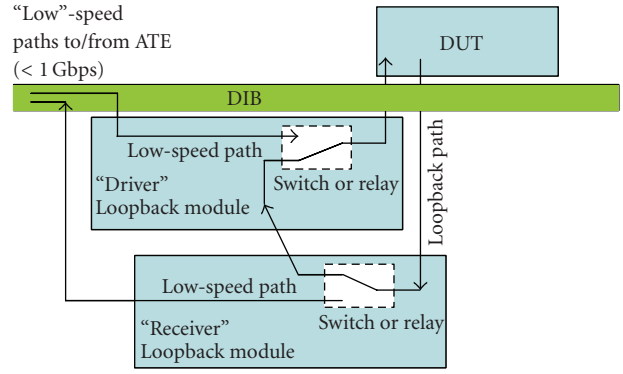

Figure 8: Two-card *passive* loopback switch arrangement. These loopback modules are "drop-in" replacements for active driver and receiver modules.

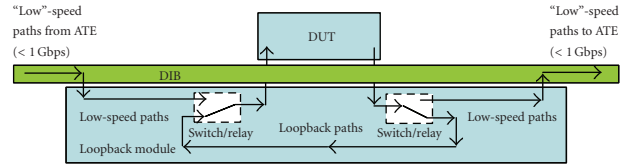

Figure 9: Single-card *passive* loopback switch arrangement. A customized single-card arrangement provides a more efficient (higher-performance) loopback path.

power dissipation, but also allows the total module thickness to be reduced by about 1/4 inch, freeing up space for more modules under the DIB.

4. PASSIVE LOOPBACK MODULE PERFORMANCE

In this section, we demonstrate the performance of several "passive" loopback cards, beginning with a 2-card arrangement (as in Figures 6 and 7), comparing cards built with mechanical RF relays to those using MEMS. We also demonstrate a single-card configuration (as shown in Figure 9) which uses MEMS.

Figure 10 shows the performance of an individual passive loopback card designed for the 2-card configuration (Figure 8). Here the data eye diagram is shown at 3.2 Gbps and 5.0 Gbps. There is a clear degradation of the data eye above 3.2 Gbps. We have determined that this is due to a combination of factors, including dielectric loss, skin effect loss, losses within the relays and small impedance discontinuities in the signal path. Channel-to-channel *skew was less than 10 picoseconds*. The losses are even more evident when both driver and receiver loopback cards are operated together, as shown in Figure 11.

In order to check the performance of the MEMS switches, we built a new passive loopback card using these in place of the mechanical relays (otherwise the designs were very similar to that shown in Figures 7 and 8). The new card using MEMS exhibited similar performance to the earlier design as shown in Figure 12 (compare to Figure 10). Although the jitter and loss characteristics are similar to those of

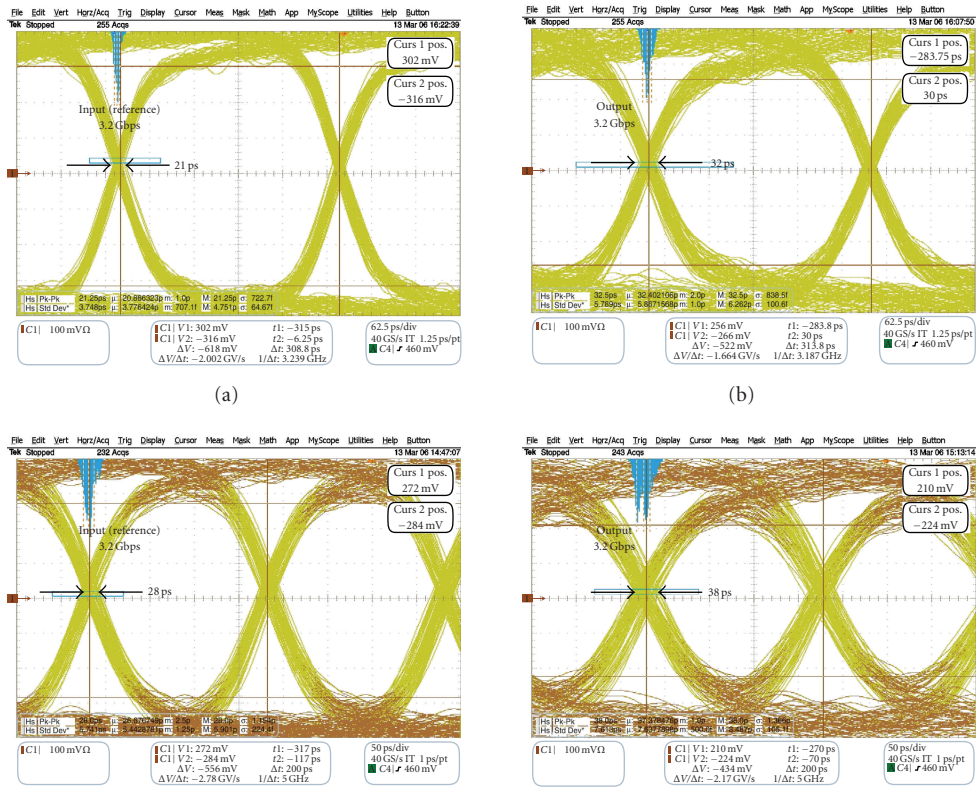

FIGURE 10: Individual card performance of a 2-card passive loopback configuration, using *mechanical RF relays*.

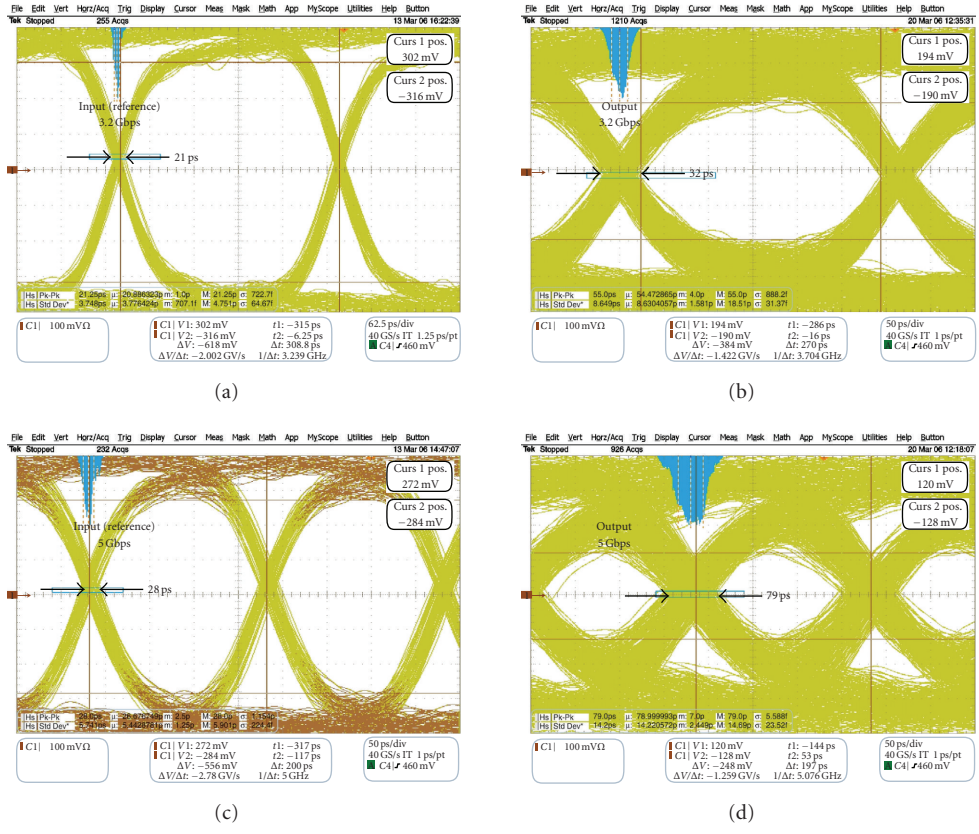

FIGURE 11: Full 2-card performance using *mechanical relays*.

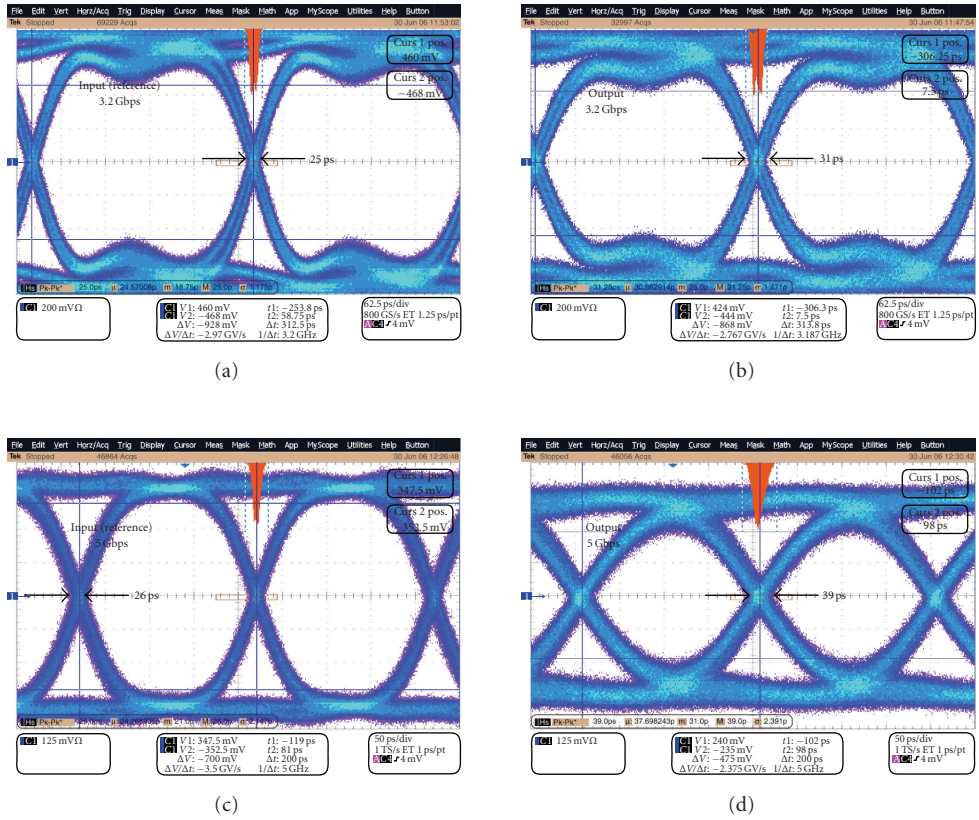

FIGURE 12: Individual card performance of a 2-card passive loopback configuration, *using MEMS relays* (compare to Figure 10).

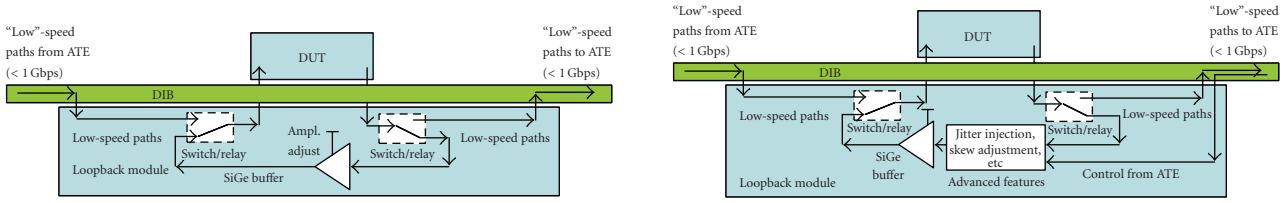

FIGURE 13: (a) The basic *active* loopback configuration and (b) active loopback with advanced features.

the mechanical relay card, there is a big improvement in power dissipation (much lower) and a significant reduction in module thickness.

Even though these passive loopback cards were able to pass data at rates up to 5 Gbps and beyond, the signal amplitude was increasingly attenuated above 3.2 Gbps. To provide full performance at higher rates required the use of *active* circuits, as shown in the next section.

5. ACTIVE LOOPBACK MODULE PERFORMANCE

As we saw in Section 4, the performance of passive loopback cards is somewhat limited by the dielectric and skin-effect losses. In some applications these losses are realistic and/or can be tolerated (i.e., when the input receivers have high sensitivity). However, in other cases we desire to recover the full amplitude signal before transmitting back to the DUT. This requires an *active* circuit, typically a buffer or amplifier. If a variable amplitude buffer/amplifier is used, then we can adjust the amplitude to emulate either small- or large-signal situations. For instance, this can be used to measure or screen for input sensitivity.

This basic "active loopback" configuration is shown in Figure 13(a). In our cards we have utilized commercially-available SiGe buffers with variable amplitude adjustment (100 mV to 700 mV) in order to handle data rates up to ~7 Gbps. Only about 10 picoseconds of skew is introduced throughout this range. We can also include features such as jitter injection, preemphasis, skew adjustment, and so forth depending on the type of testing required. This is illustrated

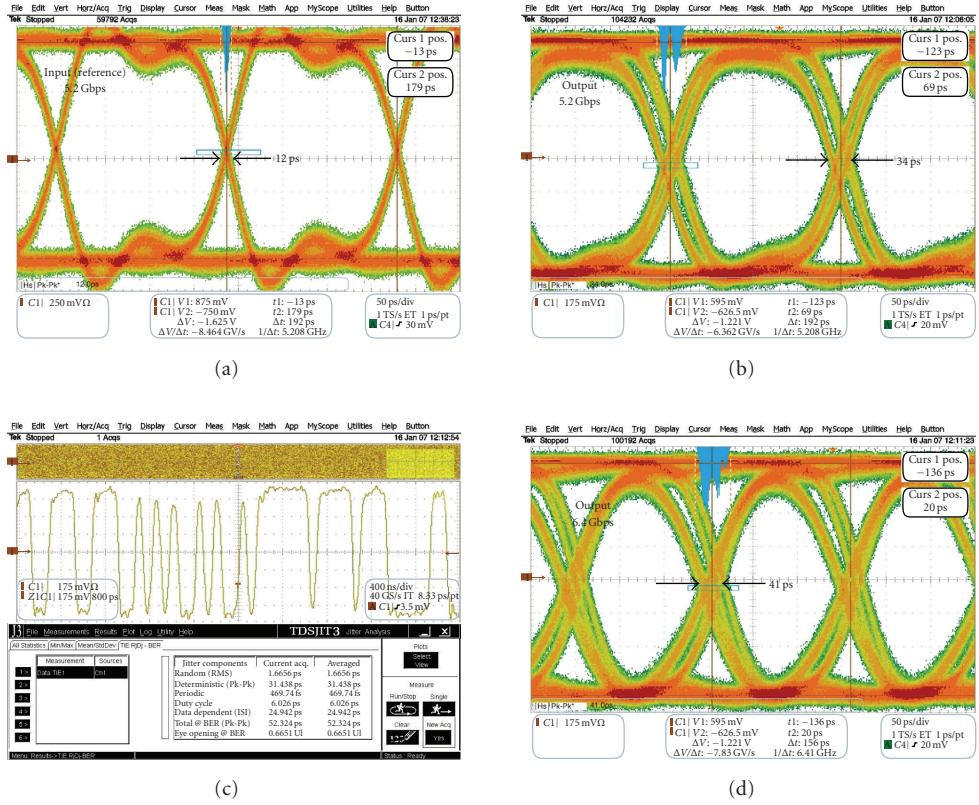

Figure 14: HyperTransport3 active loopback performance at 5.2 Gbps and 6.4 Gbps. Jitter analysis is at 6.4 Gbps.

in Figure 13(b). Such features may be implemented in future designs using SiGe logic technology.

To support HyperTransport3 loopback testing, we have constructed a 16-channel active loopback card, with each channel having a variable-amplitude differential SiGe buffer (as in Figure 13(a)). The entire card has an adjustable DC offset for matching to the DUT characteristics.

The typical performance (data eye diagrams) for one of the HyperTransport3 active loopback channels is shown in Figure 14 for both 5.2 Gbps and 6.4 Gbps. It can be seen that this card provides exceptionally good performance up to the target test rate of 5.2 Gbps and even to 6.4 Gbps. The channels add about 22 picoseconds to the total jitter. A detailed jitter analysis shows that RJ = 1.66 picoseconds, DJ = 31 picoseconds, and TJ = 52 picoseconds at BER = 10^{-12}.The card actually functions up to 8.0 Gbps, with gradually degrading data eyes above 6.4 Gbps. We have measured *channel-to-channel skew* across all 16 channels to be *less than 10 picoseconds*.

6. LIMITATIONS AND DISCUSSIONS

While the loopback cards demonstrated here met their target performance objectives, between 3.2 and 6.4 Gbps, it is clear that more work is required to handle higher rates (10 Gbps and above). Even with our best efforts, we are not able to completely eliminate jitter. As we increase frequency, the significance of "small" jitter increases and can pose the limiting obstacle to achieve these speeds. Future development is required to realize some "advanced" loopback features that we have suggested, such as jitter injection, deskew, preemphasis, and so forth.

As small as the current MEMS switch is, it is still not small enough for extreme applications involving hundreds of loopback channels. On the other hand, the fundamental MEMS technology lends itself to higher levels of integration, which therefore promises to solve this problem in the near future. Also, a higher-performance MEMS switch has recently been introduced by TeraVicta that has <0.4 dB insertion loss from DC to >20 GHz [8]. This level of performance will be required for loopback testing above 10 Gbps.

7. CONCLUSIONS

In this paper, we have shown that loopback testing of multi-Gigahertz devices can be enhanced by using MEMS switches and SiGe logic devices. The modular approach provides a high degree of flexibility. Achieving low-distortion signals at 5 Gbps and 6.4 Gbps requires careful attention to details within the module design, including the choice of relays, connectors, and logic components. Very careful attention to transmission line design is necessary to achieve picosecond delay matching and impedance matching. Newly developed

MEMS switches provide higher bandwidth and smaller size compared to traditional relays. Readily available SiGe logic can be used to configure a variety of active loopback structures that exhibit minimal losses up to 6.4 Gbps.

ACKNOWLEDGMENTS

This work was conducted as a joint R&D project between Georgia Tech and IBM Canada. The authors are grateful to IBM engineers for their efforts in designing, constructing, and testing the thermal management systems. The system-level experiments, characterization, and debug were conducted using equipment at the IBM Canada facility.

REFERENCES

[1] D. C. Keezer, D. Minier, and M.-C. Caron, "A production-oriented multiplexing system for testing above 2.5 Gbps," in *Proceedings of the IEEE International Test Conference (ITC '03)*, vol. 1, pp. 191–200, Charlotte, NC, USA, October 2003.

[2] D. C. Keezer, D. Minier, M. Paradis, and F. Binette, "Modular extension of ATE to 5 Gbps," in *Proceedings of the IEEE International Test Conference (ITC '04)*, pp. 748–757, Charlotte, NC, USA, October 2004.

[3] D. C. Keezer, D. Minier, and M.-C. Caron, "Multiplexing ATE channels for production testing at 2.5Gbps," *IEEE Design & Test of Computers*, vol. 21, no. 4, pp. 288–301, 2004.

[4] D. C. Keezer, D. Minier, and P. Ducharme, "Source-synchronous testing of multilane PCI Express and HyperTransport buses," *IEEE Design & Test of Computers*, vol. 23, no. 1, pp. 46–57, 2006.

[5] T. Kamgaing, K. Ichikawa, X. Y. Zeng, K.-P. Hwang, Y. Min, and J. Kubota, "Future package technologies for wireless communication systems," *Intel Technology Journal*, vol. 9, no. 4, pp. 353–364, 2005.

[6] K. F. Harsh, W. Zhang, V. M. Bright, and Y. C. Lee, "Flip-chip assembly for Si-based RF MEMS," in *Proceedings of the 12th IEEE International Micro Electro Mechanical Systems (MEMS '99)*, pp. 273–278, Orlando, Fla, USA, January 1999.

[7] S. Majumder, N. E. McGruer, G. G. Adams, P. M. Zavracky, R. H. Morrison, and J. Krim, "Study of contacts in an electrostatically actuated microswitch," *Sensors and Actuators A*, vol. 93, no. 1, pp. 19–26, 2001.

[8] D. A. Goins, R. D. Nelson, and J. S. McKillop, "Design of a 20 GHz low loss ohmic contact RF MEMS switch," in *Proceeding of the IEEE MTT-S International Microwave Symposium (IMS '07)*, pp. 371–374, Honolulu, Hawaii, USA, June 2007.